Appendix (Supporting Information) for

Western Boundary Current in relation to Atlantic Subtropical Gyre dynamics during abrupt glacial climate fluctuations

Dirk Nürnberg[1], Tabitha Riff[1], André Bahr[2], Cyrus Karas[3], Karl Meier[2], Jörg Lippold[2]

[1]GEOMAR Helmholtz Centre for Ocean Research Kiel, Wischhofstr. 1-3, D-24148 Kiel, Germany

[2]Institute of Earth Science, Heidelberg University, Im Neuenheimer Feld 234, D-69120 Heidelberg, Germany

[3]Universidad de Santiago, Av. B. O'Higgins 3363, Santiago, Chile

Correspondence to: Dirk Nürnberg (dnuernberg@geomar.de)

Introduction

The following part includes text passages, figures, and data tables supporting the abovementioned study. The text discusses in higher detail the ecology of the selected foraminiferal species, and diverse aspects relevant to the Mg/Ca-paleo thermometry. We also provide support for the observed cyclicity in the subSST$_{Mg/Ca}$-record. We document the age model modifications we made on the reference subSST$_{Mg/Ca}$-dataset of Parker et al. (2015).

1. **Text A.1** (text01.txt) Supporting information on foraminiferal species selected and their ecology, analytical details and error assessment for foraminiferal Mg/Ca, contamination and calcite dissolution issues, and references.
2. **Fig. A.1** (fs01.eps) Seasonal temperatures [°C] and salinities [psu] for the upper ~800 m water depth.
3. **Fig. A.2** (fs02.eps) Stable oxygen and carbon isotope signatures of *G. truncatulinoides* specimens from core 235.

4. **Fig. A.3** (fs03.eps) Comparison of temperature calibrations available for *G. truncatulinoides*.
5. **Fig. A.4** (fs04.eps) Contamination plots.
6. **Fig. A.5** (fs05.eps) Downcore Mg/Ca$_{G.truncatulinoides}$.
7. **Fig. A. 6** (fs06.eps) The frequency spectrum of the core 235 subSST$_{Mg/Ca}$ record.
8. **Fig. A.7**. (fs07.eps) Comparison of Tobago and Bonaire basins subSST$_{Mg/Ca}$ records on consistent chronologies.
9. **Table A.1** (ts01.txt) Age control for Tobago Basin core 235 .

Text A.1. Supporting information on foraminiferal species selected and their ecology, analytical details and error assessment for foraminiferal Mg/Ca, contamination and calcite dissolution issues, and references.

Ecology of the selected foraminiferal species

To reconstruct subsurface ocean properties, we selected calcitic tests of the planktonic foraminiferal species *Globorotalia truncatulinoides* (d´Orbigny, 1839). *G. truncatulinoides* is a deep-dwelling, subtropical species, which is adopted to a wide range of water temperatures and salinities (Lohmann and Schweitzer 1990). Its stratigraphic range is from early Pleistocene to today (Kennett and Srinivasan, 1983). *G. truncatulinoides* exhibits a complex life cycle, beginning in the upper meters of the water column. It continues to grow and calcify new chambers at greater water depth until it reaches its adult stage, apparently pursuing a reproductive strategy that requires annual vertical migration of several hundred meters, with greater living depths during spring and summer (Cléroux et al., 2009). Sediment trap time series in the northern Gulf of Mexico demonstrate that 92% of its flux occurs from January to March (Reynolds et al., 2018). In the Atlantic and the Caribbean, the habitat depth range of *G. truncatulinoides* is from 0 m to >400 m) (e.g. Cléroux et al., 2008; Jentzen et al., 2018b; Schmuker and Schiebel, 2002; Steph et al., 2009). Encrustation stages, however, may reflect calcification at different depths (Reynolds et al., 2018). Non-encrusted and encrusted specimens reveal mean calcification depths of 66 ± 9 m (with a range between 0-150 m) and 379 ± 76 m (with a range between 170 and 700 m), respectively (Reynolds et al., 2018). In the eastern Caribbean, *G. truncatulinoides* apparently prefers a habitat at 180-300 m (Jentzen et al., 2018b) (c.f. Fig. A.1).

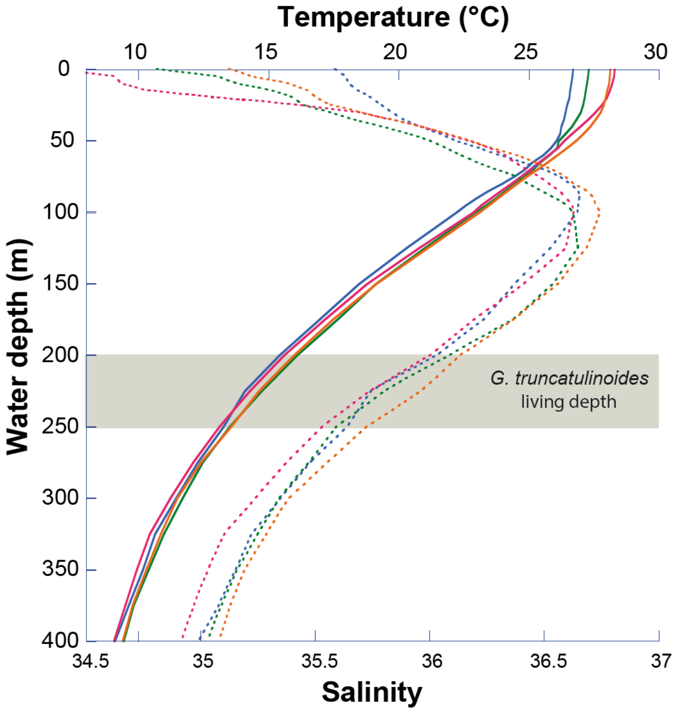

Fig. A.1. Seasonal temperatures [°C] and salinities [psu] for the upper ~800 m water depth (WOA Station 25458 at 11.5°N 60.5°W; Locarnini et al., 2018). Solid and stippled lines denote the temperature and salinity profiles, respectively: Jan.-Mar. (blue), Apr.-Jun. (green), Jul.-Sep. (red), Oct.-Dec. (orange). Gray shading marks the assumed living depth of *G. truncatulinoides* according to Jentzen et al. (2018a).

As the majority of the *G. truncatulinoides* specimens in core 235 are encrusted (c.f. Fig. A.2), and as the core 235 location is closer to the eastern part of the Caribbean, we assume a habitat depth range of ~200-250 m. This corresponds to a depth nearly below the main thermocline in Tobago Basin (180-220 m) (Locarnini et al., 2018) and is in good agreement with the findings of Jentzen et al. (2018b).

G. truncatulinoides shows a coiling dimorphism, separating this species into sinistral (left-coiled) and dextral (right-coiled) morphotypes. The preferred habitats of both morphotypes, however, are rather similar (Jentzen et al., 2018b; Cléroux et al., 2008). Following Friedrich et al. (2012) and Ganssen and Kroon (2000), who showed that both morphotypes have similar stable oxygen isotopic (δ^{18}O), carbon isotopic (δ^{13}C) and Mg/Ca signatures, we did not differentiate between coiling directions. Ujiié et al. (2010) further showed that the dextral form is dominant at our core 235 location.

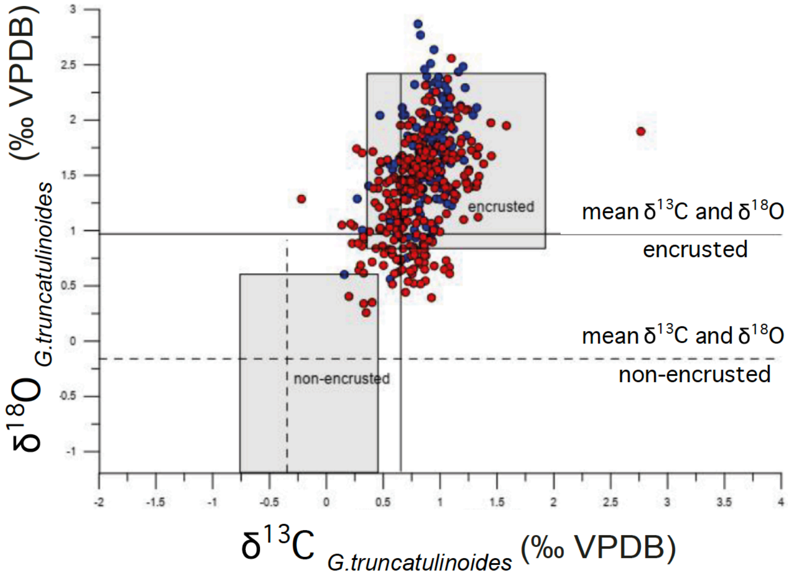

Fig. A.2. Stable oxygen and carbon isotope signatures of *G. truncatulinoides* specimens from core 235. The δ^{13}C and δ^{18}O data (in ‰ vs. VPDB) of this study are in blue, while the associated Reißig et al. (2019) data are in red, all measured on the same mass spectrometer (c.f. Chapter 3.3.1). The gray shaded fields denote data ranges and means for either encrusted or non-encrusted specimens (Reynolds et al., 2018). In this study, most specimens selected for geochemical analyses are encrusted individuals.

Calcitic tests of the foraminiferal species were hand-picked under a binocular microscope. The size fraction had to be enlarged to 250-400 µm due to insufficient sample material. Friedrich et al. (2012) stated that *G. truncatulinoides* has no size effect on Mg/Ca. Also, δ^{13}C and δ^{18}O show no systematic changes in the selected size fraction (Elderfield et al. 2002). For the isotope-geochemical studies, ~30 species-specific foraminiferal tests per sample were gently crushed between cleaned glass plates to open the chambers for efficient cleaning. Over-crushing was avoided to prevent an excessive sample loss during cleaning procedure. The fragments of the tests were homogenized and split into subsamples for stable isotope (one third) and trace metal analyses (two thirds) and transferred into cleaned vials. Chamber fillings (e.g. pyrite, clay) and other contaminant phases (e.g. conglomerates of metal oxides) were thoroughly removed before chemical cleaning and analyses. All analytical data are available online at the Data Publisher for Earth and Environmental Science, PANGEA (www.pangaea.de): https://doi.org/10.1594/PANGAEA.919497.

Foraminiferal Mg/Ca-paleo thermometry

Over the past decades, foraminiferal Mg/Ca has been proven to be a robust, reliably precise, and reproducible proxy for ocean temperatures (e.g., Elderfield and Ganssen, 2000; Lea et al., 1999; Nürnberg, 1995, 2000; Nürnberg et al., 1996). To prepare the foraminiferal samples for elemental analyses, the foraminiferal tests were intensively cleaned oxidatively and reductively (with hydrazine) following the protocols from Boyle and Keigwin (1985/86) and Boyle and Rosenthal (1996). This procedure was similarly applied by Reißig et al. (2019) on core 235 foraminiferal sample material, and allows direct comparison of analytical results.

Trace metal analyses were performed on a VARIAN 720-ES Axial ICP-OES, a simultaneous, axial-viewing Inductively Coupled Plasma - Optical Emission Spectrometer coupled to a VARIAN SPS3 sample preparation system. To assure analytical quality control the measurement strategy involved the regular analyses of standards and blanks. The results were normalized to the ECRM 752-1 standard (3.761 mmol/mol Mg/Ca; Greaves et al., 2008) and were drift corrected. The external reproducibility for the ECRM standard was ±0.01 mmol/mol for Mg/Ca (2σ SD). Replicate measurements reveal a reproducibility of ±0.28 mmol/mol for *G. truncatulinoides* (2σ SD).

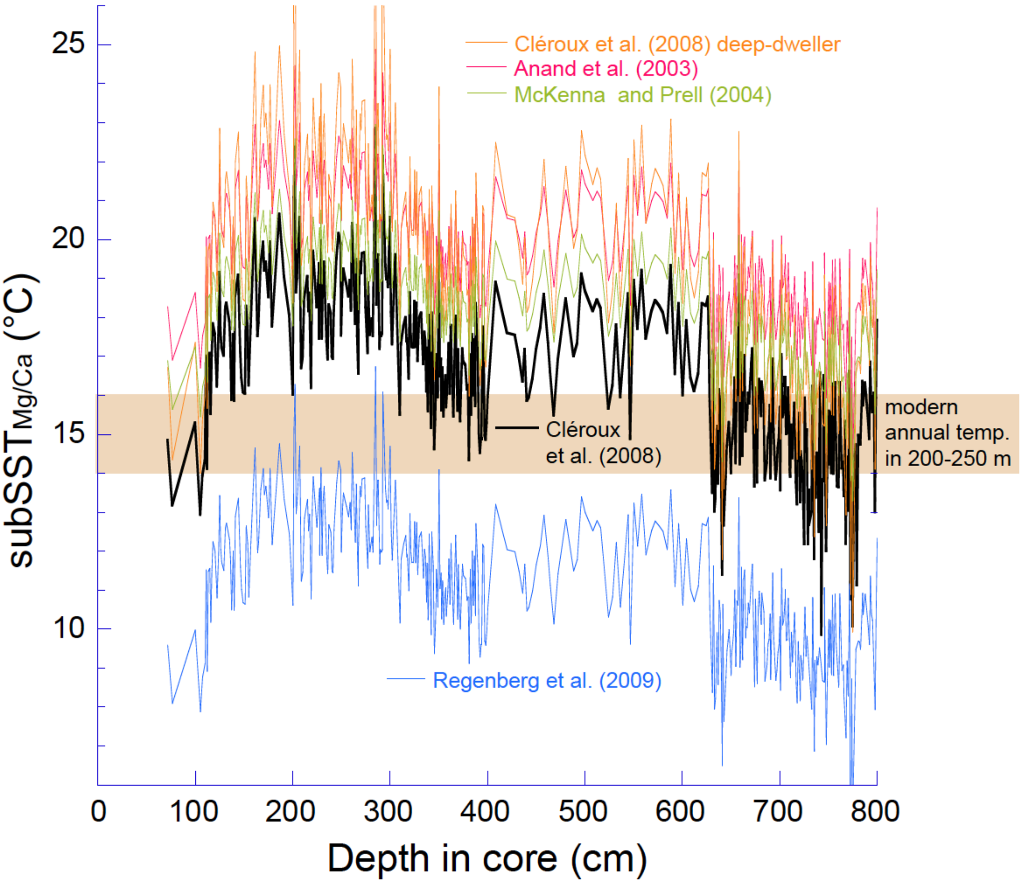

Fig. A.3. Comparison of temperature calibrations available for *G. truncatulinoides*. Calibrations of Cléroux et al. (2008) (dextral morphotype) and Cléroux et al. (2008) (deep-dweller) were considered most reliable (black and orange) to convert Mg/Ca$_{\textit{G.truncatulinoides}}$ into subSST$_{\text{Mg/Ca}}$. Other calibrations from Anand (2003; red), Regenberg et al. (2009; blue; deep-dweller) and McKenna and Prell (2004; green) were not applied, as they provide too warm or too cool core-top subSST$_{\text{Mg/Ca}}$. Brown-shading indicates modern annual temperatures at 200-250m water depth in Tobago Basin (c.f. Fig. A.1).

For *G. truncatulinoides*, there is a variety of calibration equations available to convert the foraminiferal Mg/Ca ratios into paleotemperatures (c.f. Fig. A.3). The Mg/Ca$_{\textit{G.truncatulinoides}}$ ratios were converted into subsurface temperatures (termed subSST$_{\text{Mg/Ca}}$) using the exponential calibration equation of Cléroux et al. (2008) established from widely distributed Atlantic sample material: Mg/Ca = 0.62 $\pm$ 0.16 exp(0.74 $\pm$ 0.017 * T). We finally applied the calibration for the dextral morphotype (s. above). When applying the calibration equation of Cléroux et al. (2008), the calculated latest Holocene subSST$_{\text{Mg/Ca}}$ of ~14.9°C (Reißig et al., 2019) matches the modern annual subsurface temperatures of 14-15°C at 200-250 m depth (Locarnini et al., 2018). With the asserted reproducibility of 0.28 mmol/mol, the error (2σ) of calculated subSST$_{Mg/Ca}$ is ± 0.71°C. In order to achieve consistency between our datasets and published reference datasets from Bonaire Basin, we recalculated the Parker et al. (2015) subSST$_{Mg/Ca}$ data derived from Mg/Ca$_{G.truncatulinoides}$ ratios using the Cléroux et al. (2008) calibration. This led to consistently lower-by-4°C subSST$_{Mg/Ca}$ for the glacial time period then previously published by Parker et al. (2015), who used the Anand et al. (2003) calibration. Reißig et al. (2019) in detail discussed the appropriateness of the Cléroux et al. (2008) calibration.

Analytical outliers and contamination effects

A small number of single trace metal analyses from 670 cm, 683 cm, 714 cm, 755.5 cm, 763 cm and 770.5 cm core depths were removed from the core 235 dataset as they yielded extremely high/low element/Ca values compared with the surrounding data, and the according Mg/Ca data led to unrealistically high or low subSST$_{Mg/Ca}$ values. The Mg/Ca data (2.65, 0.88, 4.14, 1.99, 1.29, 1.28 mmol/mol) were accompanied by high Al/Ca (0.7, 0.12, 0.49, 1.14, 0.94, 2.34 mmol/mol) and Fe/Ca (0.18, 0.06, 0.16, 0.27, 3.39, 0.03 mmol/mol) ratios, (c.f. Fig. A.4).

By monitoring the remaining foraminiferal samples for their Fe/Ca, Al/Ca and Mn/Ca ratios, the effect of cleaning efficiency, post depositional contamination, and diagenetic alteration on foraminiferal Mg/Ca was examined. Contamination-indicative threshold values exist for Fe/Ca, Al/Ca and Mn/Ca ratios (<0.1 mmol/mol; Barker et al., 2003; Them et al., 2015). Numerous studies have shown meanwhile that the Barker et al. (2003) threshold values - defined in the North Atlantic - are often exceeded as they largely depend on the sediment type the foraminiferal tests were removed from (Nünberg et al., 2015). The Al/Ca, Fe/Ca and Mn/Ca ratios in our foraminiferal samples are often higher than the given threshold values, and at times reach values of up to ~1.1 mmol/mol, ~0.7 mmol/mol, and ~0.22 mmol/mol, respectively (Fig. A.4, A.5). It needs to be noted, in this respect, that these high contaminant values do not consistently have extraordinary foraminiferal Mg/Ca ratios. Also, the correlation of Mg/Ca to either Fe/Ca, Al/Ca or Mn/Ca (R^2 = 0.15, R^2 = 0.19; R^2 = 0.06) is insignificant, suggesting that samples were not contaminated. A high covariance between Mg/Ca and Mn/Ca, Fe/Ca and/or Al/Ca would imply insufficient clay removal during cleaning (Barker et al., 2003).

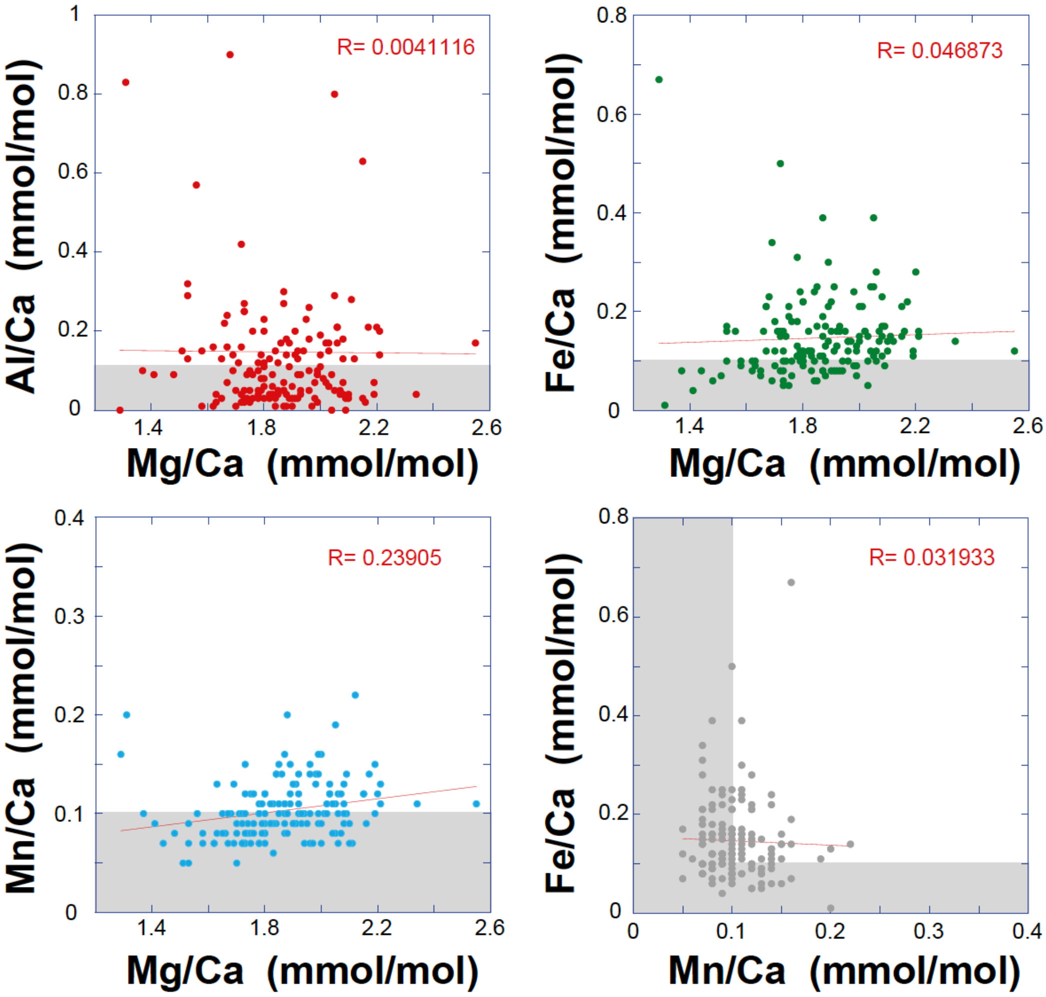

Fig. A.4. Contamination plots. Foraminiferal Mg/Ca vs. Al/Ca (red), Fe/Ca (green), Mn/Ca (blue) reveal only low correlation coefficients (R) for *G. truncatulinoides*. Al/Ca, Fe/Ca and Mn/Ca partly exceed threshold values (>0.1 mmol/mol, gray shading) proposed by Barker et al. (2003). Mn/Ca vs. Fe/Ca is not correlated, implying no ferromanganese coating.

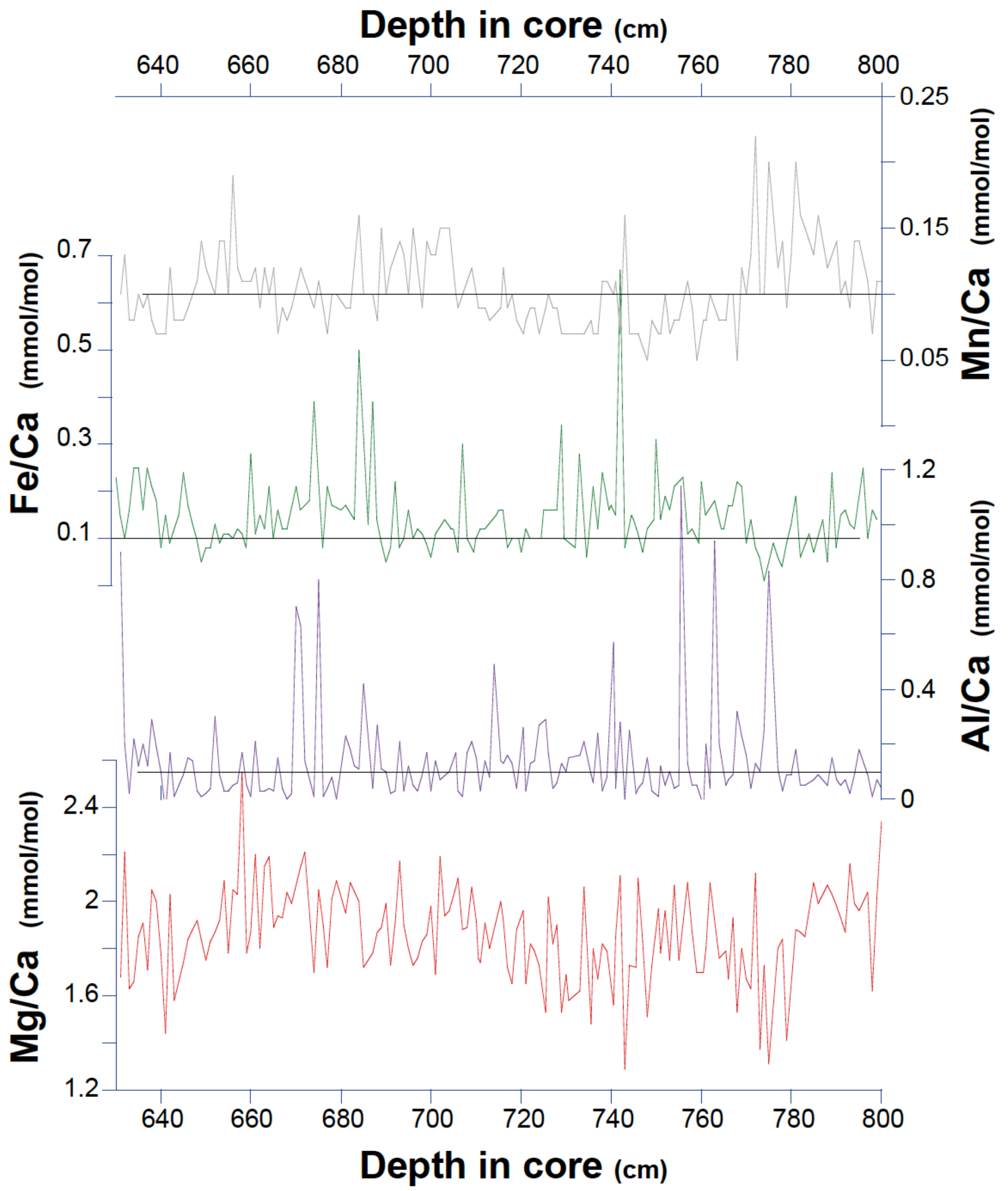

Fig. A.5. Downcore Mg/Ca$_{G.truncatulinoides}$ of Tobago Basin core 235 (red) in comparison to contaminant elemental ratios Al/Ca (blue), Fe/Ca (green), and Mn/Ca (gray) from the same samples. Correlation coefficients are given in Fig. A4. Threshold values indicative of sample contamination (>0.1 mmol/mol) suggested by Barker et al. (2003) and Them et al. (2015) are indicated by horizontal dashed lines, but should be viewed cautiously.

Furthermore, there is no indication that the record of *G. truncatulinoides* is contaminated by Fe-Mn-coatings, which have effects on Mg/Ca. There is no statistically significant positive correlation between Mn/Ca and Fe/Ca (Fig. A.4). Also, foraminiferal samples showing particularly high Mn/Ca ratios are rather low in Fe/Ca (Fig. A.5) suggesting that the foraminiferal Mg/Ca values are not biased by Fe/Mn coatings. According to Roberts et al. (2016), a foraminiferal Mg/Mn ratio of 0.1 mol/mol within a diagenetic coating would account for 10^{-2} mmol/mol at maximum to foraminiferal Mg/Ca, which is well within the reproducibility of the Mg/Ca analyses. In our dataset, the Mg/Mn within foraminiferal tests is on average 0.02±0.005 mol/mol). We hence conclude that sample contamination due to diagenetic coatings is negligible to our Mg/Ca analyses.

When cracking the foraminiferal tests, partially golden to silver colored crystalline particles at the inner chamber walls were observed. These crystalline particles were identified as pyrite (FeS_2), which forms in marine sediments by the activity of sulphate-reducing bacteria under suboxic conditions. Elevated Fe/Ca ratios may reflect the presence of pyrite during the measurements, although brushing of test walls before cleaning, and the intense cleaning steps including nitric acid, to which pyrite is soluble, were considered sufficient enough to remove most of the pyrite coatings. Nürnberg et al. (2015) concluded from samples with high pyrite content from off Peru that even the measured high Fe/Ca ratios (4.08 mmol mol^{-1}) did not affect the Mg/Ca signal.

Dissolution effects on foraminiferal Mg/Ca

It is important to rule out calcite dissolution effects on foraminiferal Mg/Ca, preferentially controlled by the calcite-saturation state of the bottom waters. Regenberg et al. (2006) showed that Mg/Ca starts to decline linearly below $\Delta[CO_3^{2-}]$ levels of ~18-26 µmol/kg. Later, Regenberg et al. (2014) defined a global critical threshold for dissolution of 21.3 ± 6.6 µmol/kg $\Delta[CO_3^{2-}]$. In Tobago Basin, this threshold value is at a depth of ~3500 m (Regenberg et al., 2014). As core 235 is from ~825 m water depth we assess calcite dissolution unlikely to have affected foraminiferal Mg/Ca. Further discussions on this issue can be found in Poggemann et al. (2017; 2018) and Reißig et al. (2019).

Spectral analysis of subSST$_{Mg/Ca}$ >32.8 ka BP

Based on the established age model, we observe that the highly-variable subSST$_{Mg/Ca}$-record >32.8 ka BP does not follow the D/O-related stadial-interstadial variability. The proxy record, however, is characterized by high-frequency variations, and subSST$_{Mg/Ca}$-maxima occur during stadials and during transitional periods (Fig. 4B). In order to test whether these variations are cyclic, we ran a B-Tukey test (AnalySeries 2.0; Paillard et al., 1996) on the subSST$_{Mg/Ca}$-record >32.8. The according core section from 631 cm to 800 cm core depth showing a sedimentation rate of ~62 cm/kyr was sampled each 1 cm, providing an average temporal resolution of ~20 (+/-15) years of the proxy-record. Dominant ~740 year-cycles were revealed in the B-Tukey frequency spectrum of the 5 point-smoothed subSST$_{Mg/Ca}$ record (Fig. 4B; Fig. A.6) (using a Bartlett window; bandwidth = 0.00110327; error on the power spectrum is $0.511144 < \Delta\text{Power} / \text{Power} < 3.00024$). This periodicity not only suggests a regular pacing of the tropical West Atlantic ocean system. It also corroborates the validity of our core chronology, as the ~740 year-periodicity is half of the well-known Dansgaard-Oeschger cycles of 1.470 years (Rahmstorf, 2003).

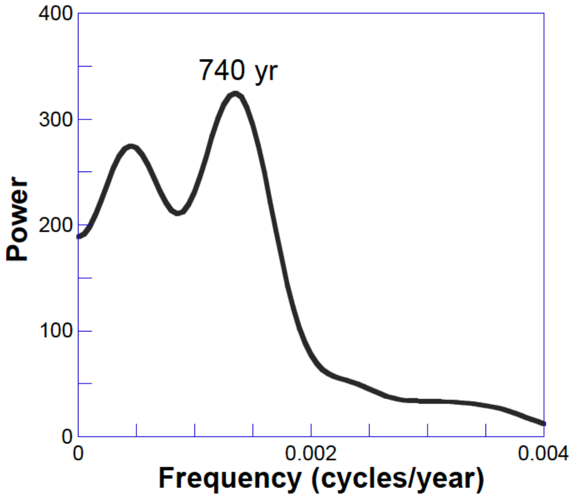

Fig. A. 6. The frequency spectra of the core 235 subSST$_{Mg/Ca}$ record from 37-32.8 ka BP (Fig. 4B) reveals a dominant cyclicity of 740 years, which is half a Dansgaard-Oeschger cycle.

Modified age model for reference core VM12-107 from Bonaire Basin for better comparison

In our study, we attempted to achieve a convincing comparison between our Tobago Basin core 235 $\text{subSST}_{\text{Mg/Ca}}$ record to a similar record of adjacent Bonaire Basin core VM12-107 (Parker et al., 2015). Although both are well-dated records on D/O stadial/interstadial timescales, the comparison is complicated by the fact that the core 235 AMS^{14}C-chronology is based on the new MARINE20 marine reservoir correction database (Stuiver et al., 2020; http://calib.org), while that of core VM12-107 is not. We hence re-calibrated the AMS^{14}C-datings of core VM12-107 (Parker et al., 2015; Schmidt et al., 2012) by using MARINE20, and by applying a reservoir age correction of -130 ± 55 years (Hughen et al., 2004) valid for nearby Caraico Basin. The deviation in initial and modified age models is within decades, but allows a better comparison to the core 235 age model in particular for the time period of rapid D/O stadial-interstadial change from 37-30 ka BP (Fig. A.7).

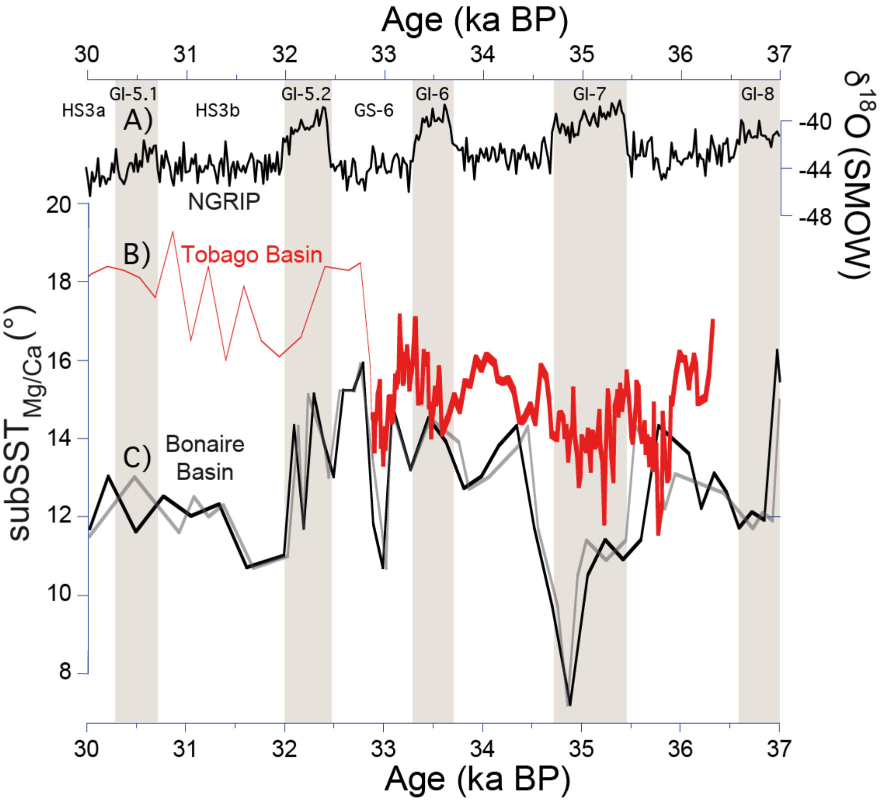

Fig. A.7. Comparison of Tobago and Bonaire basins subSST$_{Mg/Ca}$ records on consistent chronologies. A) Greenland ice core $\delta^{18}O$ record as reference for the northern hemisphere climate signal (NGRIP Dating Group, 2006). B) subSST$_{Mg/Ca}$ record from Tobago Basin (this study). C) subSST$_{Mg/Ca}$ record from Bonaire Basin on the original (Parker et al., 2015; gray) and on the revised age model (this study; black). In order to guarantee compatibility to core 235, the initial AMS^{14}C-datings (31960 yr BP, 33060 yr BP, 35690 yr BP) of Parker et al. (2015) were re-calibrated using the new MARINE20 dataset (Stuiver et al., 2020). The AMS^{14}C-datings were changed to 31872 yr BP, 33073 yr BP, and 35949 yr BP, applying a reservoir age of ΔR = -130 ± 55 years (Hughen et al., 2004; www.calib.org) taken from nearby Caraico Basin.

Table A.1. Age control for Tobago Basin core 235. The age model is primarily based on the linear interpolation between Accelerator Mass Spectrometry (AMS) radiocarbon (^{14}C) dates, analyzed by Cologne AMS (Germany) (Reißig et al., 2019), by Beta Analytic Radiocarbon Dating Laboratory (UK) (Hoffmann et al., 2014; Poggemann et al., 2017), and at the University of Bern following the methodology described by Gottschalk et al. (2018) (this study). Calibrated AMS^{14}C ages using Calib 7.1 software and the new MARINE20 database were calculated by taking in consideration a local reservoir age of 550 yrs (ΔR= -161 ± 24 yrs; Stuiver et al., 2020; http://calib.org). The previously published AMS^{14}C ages (in brackets, black) were still calibrated with MARINE13. Further improvement of the age model was derived by graphically tuning the benthic $\delta^{18}O_{Uvigerina}$ record of core 235 to the high-resolution North Greenland Ice core Project (NGRIP) $\delta^{18}O$ reference record (NGRIP Dating Group, 2006). Thereby, two additional tielines became necessary in order to improve the match of benthic $\delta^{18}O_{Uvigerina}$ minima and Greenland stadials (c. f. Fig. 2).

Core 235	**Lab code**	**^{14}C Age**	**Age error**	**Median**	**Remark**	**Lower**	**Upper**	**Error**	**Lower**	**Upper**	**Error**	**POINTER**	**Refe-rence-**
Depth	**AMS^{14}C**	**(yrs BP)**	**+/- (yrs)**	**probab.**		**range**	**range**	**1σ**	**range**	**range**	**2σ**	**age (yrs BP)**	
(cm)				**(yrs BP)**		**(yrs BP)**	**(yrs BP)**	**(yrs)**	**(yrs BP)**	**(yrs BP)**	**(yrs)**	**(yrs BP)**	
3	COL1473.1.1	569	31	185 (242)	AMS^{14}C	110	273	163	0	313	313	**225**	Hoffmann et al. 2014
43	COL1474.1.1	2926	32	2719 (2732)	AMS^{14}C	2643	2797	154	2530	2868	338	**2719**	Hoffmann et al. 2014
133	COL1475.1.1	8424	44	9036 (9063)	AMS^{14}C	8935	9137	202	8824	9255	431	**9131**	Hoffmann et al. 2014
188	COL1476.1.1	10500	48	11820 (11757)	AMS^{14}C	11694	11940	246	11558	12092	534	**11795**	Hoffmann et al. 2014
218	COL1477.1.1	11586	48	13068 (13103)	AMS^{14}C	12983	13156	173	12880	13240	360	**13119**	Hoffmann et al. 2014
298	COL1478.1.1	13098	49	15115 (15158)	AMS^{14}C	14996	15229	233	14873	15358	485	**15220**	Hoffmann et al. 2014
317	BETA-453718	12920	40	14881	not considered	14771	15023	252	14575	15118	543		this study
326		13850	60	16098 (16213)	AMS^{14}C	15967	16233	266	15818	16365	547	**16018**	Poggemann et al. 2017
358	COL1479.1.1	15959	57	18624 (18832)	AMS^{14}C	18518	18765	247	18323	18828	505	**18667**	Poggemann et al. 2017
423	COL1480.1.1	20139	93	23475 (23793)	AMS^{14}C	23332	23664	332	23147	23756	609	**23447**	Poggemann et al. 2017
614				31999	tie line							**31999**	this study
628		29300	200	33070 (33122)	AMS^{14}C	32793	33399	606	32331	33652	1321	**32845**	Reißig et al. 2019
697	BE-10333.1.1	29471	228	33286 (33297)	AMS^{14}C	33003	33605	602	32623	33920	1297	**33596**	Reißig et al. 2019
762	BE-10334.1.1	29881	237	33734	not considered	33475	34031	556	33166	34230	1064		this study
717				34748	tie line							**34748**	this study
795	BE-10335.1.1	32637	331	36456 (33156)	AMS^{14}C	36091	36821	730	35703	37260	1557	**36172**	this study

References

Anand, P., Elderfield, H., Conte, M.H. (2003). Calibration of Mg/Ca thermometry in planktonic foraminifera from a sediment trap time series. Paleoceanography 18(2), 1050. https://doi.org/10.1029/2002PA000846.

Barker, S., Greaves, M., Elderfield, H. (2003). A study of cleaning procedures used for foraminiferal Mg/Ca paleo thermometry. Geochemistry, Geophysics, Geosystems 4 (9). https://doi.org/10.1029/2003GC000559.

Boyle, E.A., Keigwin, L.D. (1985/86). Comparison of Atlantic and Pacific paleochemical records for the last 215,000 years: changes in deep ocean circulation and chemical inventories. Earth Planetary Science Letters 76, 135-150.

Boyle, E.A., Rosenthal, Y. (1996). Chemical hydrography of the South Atlantic during the Last Glacial Maximum: Cd vs. $\delta^{13}C$. In: Wefer, G., Berger, W.H., Siedler, G., Webb, D. (eds.), The South Atlantic: Present and Past Circulation, Springer, Berlin, Heidelberg, 423-443.

Cléroux, C., Cortijo, E., Anand, P., Labeyrie, L., Bassinot, F., Caillon, N., Duplessy, J.-C. (2008). Mg/Ca and Sr/Ca ratios in planktonic foraminifera: Proxies for upper water column temperature reconstruction. Paleoceanography 23, PA3214. https://doi.org/10.1029/2007PA001505.

Cléroux, C., Lynch-Stieglitz, J., Schmidt, M.W., Cortijo, E., Duplessy, J.-C. (2009). Evidence for calcification depth change of *Globorotalia truncatulinoides* between deglaciation and Holocene in the Western Atlantic Ocean. Marine Micropaleontology 73 (1-2), 57–61.

Elderfield, H., Ganssen, G. (2000). Past temperature and $\delta^{18}O$ of surface ocean waters inferred from foraminiferal Mg/Ca ratios. Nature 405 (6785), 442–445.

Elderfield, H., Vautravers, M., Cooper, M. (2002). The relationship between shell size and Mg/Ca, Sr/Ca, $\delta^{18}O$, and $\delta^{13}C$ of species of planktonic foraminifera. Geochemistry, Geophysics, Geosystems 3 (8), 1–13.

Friedrich, O., Schiebel, R., Wilson, P.A., Weldeab, S., Beer, C.J., Cooper, M.J., Fiebig, J. (2012). Influence of test size, water depth, and ecology on Mg/Ca, Sr/Ca, $\delta^{18}O$ and $\delta^{13}C$ in nine modern species of planktic foraminifers. Earth and Planetary Science Letters 319- 320, 133–145.

Ganssen, G., Kroon, D. (2000). The isotopic signature of planktonic foraminifera from NE Atlantic surface sediments: Implications for the reconstruction of past oceanic conditions. Journal of the Geological Society 157 (3), 693–699.

Greaves, M., Caillon, N., Rebaubier, H., Bartoli, G., Bohaty, S., Cacho, I., Clarke, L., Cooper, M., Daunt, C., Delaney, M., deMenocal, P., Dutton, A., Eggins, S., Elderfield, H., Garbe- Schoenberg, D., Goddard, E., Green, D., Groeneveld, J., Hastings, D., Hathorne, E., Kimoto, K., Klinkhammer, G., Labeyrie, L., Lea, D.W., Marchitto, T., Martínez-Botí, M.A., Mortyn, P.G., Ni, Y., Nürnberg, D., Paradis, G., Pena, L., Quinn, T., Rosenthal, Y., Russell, A., Sagawa, T., Sosdian, S., Stott, L., Tachikawa, K., Tappa, E., Thunell, R., Wilson, P.A. (2008). Interlaboratory comparison study of calibration standards for foraminiferal Mg/Ca thermometry. Geochemistry, Geophysics, Geosystems 9 (8). https://doi.org/10.1029/2008GC001974.

Gottschalk, J., Szidat, S., Michel, E., Mazaud, A., Salazar, G., Battaglia, M., Lippold, J., Jaccard, S. (2018). Radiocarbon measurements of small-size foraminiferal samples with the Mini Carbon Dating System (MICADAS) at the University of Bern: Implications for paleoclimate reconstructions. Radiocarbon 60(2), 469-491. https://doi.org/10.1017/RDC.2018.3.

Hoffmann, J., Bahr, A., Voigt, S., Schönfeld, J., Nürnberg, D., Rethemeyer, J. (2014). Disentangling abrupt deglacial hydrological changes in northern South America: Insolation versus oceanic forcing. Geology 42 (7), 579–582.

Hughen, K.A, Southon, J.R, Bertrand, C.J.H, Frantz, B., Zermeno, P. (2004). Cariaco Basin calibration update: revisions to calendar and ^{14}C chronologies for core PL07-58PC. Radiocarbon 46, 1161-1187.

Jentzen, A., Nürnberg, D., Hathorne, E. C., Schönfeld, J. (2018a). Mg / Ca and δ^{18}O in living planktic foraminifers from the Caribbean, Gulf of Mexico and Florida Straits. Biogeosciences 15 (23), 7077-7095. doi:10.5194/bg-15-7077-2018.

Jentzen, A., Schönfeld, J., Schiebel, R. (2018b). Assessment of the effect of increasing temperature on the ecology and assemblage structure of modern planktic foraminifers in the Caribbean and surrounding seas. Journal of Foraminiferal Research 48 (3), 251–272. doi:10.2113/gsjfr.48.3.251.

Kennett, J.P., Srinivasan, M.S. (1983). Neogene planktonic foraminifera. A phylogenetic atlas. Hutchinson Ross, Stroudsburg, Pa.

Lea, D.W., Mashiotta, T.A., Spero, H.J. (1999). Controls on magnesium and strontium uptake in planktonic foraminifera determined by live culturing. Geochimica et Cosmochimica Acta 63 (16), 2369–2379.

Locarnini, R.A., Mishonov, A.V., Baranova, O.K., Boyer, T.P., Zweng, M.M., Garcia, H.E., Reagan, J.R., Seidov, D., Weathers, K.W., Paver, C.R., Smolyar, I.V. (2018). Temperature. NOAA Atlas NESDIS in preparation. World Ocean Atlas 2018 (1).

Lohmann, G.P., Schweitzer, P.N. (1990). *Globorotalia truncatulinoides'* growth and chemistry as probes of the past thermocline: 1. Shell size. Paleoceanography 5 (1), 55– 75.

McKenna, VS; Prell, WL (2004). Calibration of the Mg/Ca of *Globorotalia truncatulinoides* (R) for the reconstruction of marine temperature gradients. Paleoceanography 19(2), PA2006. https://doi.org/10.1029/2000PA000604.

NGRIP Dating Group (2006). Greenland Ice Core Chronology 2005 (GICC05): IGBP PAGES/World Data Center for Paleoclimatology. Data Contribution Series # 2006- 118,NOAA/NCDC Paleoclimatology Program, Boulder CO, USA.

Nürnberg, D. (1995). Magnesium in tests of *Neogloboquadrina pachyderma* sinistral from high northern and southern latitudes. Journal of Foraminiferal Research 25 (4), 350– 368.

Nürnberg, D. (2000). PALEOCLIMATE: Taking the Temperature of Past Ocean Surfaces. Science (New York, N.Y.) 289 (5485), 1698–1699.

Nürnberg, D., Bijma, J., Hemleben, C. (1996). Assessing the reliability of magnesium in foraminiferal calcite as a proxy for water mass temperatures. Geochimica et Cosmochimica Acta 60 (5), 803–814.

Nürnberg, D., Böschen, T., Doering, K., Mollier-Vogel, E., Raddatz, J., Schneider, R. (2015). Sea surface and subsurface circulation dynamics off equatorial Peru during the last ~17 kyr. Paleoceanography 30 (7), 984–999.

Paillard, D., Labeyrie, L., Yiou, P. (1996), Macintosh program performs time-series analysis, Eos Trans. AGU 77, 379.

Parker, A.O., Schmidt, M.W., Chang, P. (2015). Tropical North Atlantic subsurface warming events as a fingerprint for AMOC variability during Marine Isotope Stage 3. Paleoceanography 30 (11), 1425–1436.

Poggemann, D.-W., Hathorne, E.C., Nürnberg, D., Frank, M., Bruhn, I., Reißig, S., Bahr, A. (2017). Rapid deglacial injection of nutrients into the tropical Atlantic via Antarctic Intermediate Water. Earth and Planetary Science Letters 463, 118–126. http://dx.doi.org/10.1016/j.epsl.2017.01.

Poggemann, D.-W., Nürnberg, D., Hathorne, E.C., Frank, M., Rath, W., Reißig, S., Bahr, A. (2018). Deglacial Heat Uptake by the Southern Ocean and Rapid Northward Redistribution Via Antarctic Intermediate Water. Paleoceanography and Paleoclimatology 33 (11), 1292–1305. https://doi.org/10.1029/2017PA003284.

Rahmstorf, S. (2003). Timing of abrupt climate change: A precise clock. Geophysical Research Letters 30 (10), 1510. doi:10.1029/2003GL017115.

Regenberg, M., Nürnberg, D., Steph, S., Groeneveld, J., Garbe-Schönberg, D., Tiedemann, R., Dullo, W.-C. (2006). Assessing the effect of dissolution on planktonic foraminiferal Mg/Ca ratios: Evidence from Caribbean core tops. Geochemistry, Geophysics, Geosystems 7 (7), Q07P15. doi:10.1029/2005GC001019.

Regenberg, M., Steph, S., Nürnberg, D., Tiedemann, R., Garbe-Schönberg, D. (2009). Calibrating Mg/Ca ratios of multiple planktonic foraminiferal species with δ^{18}O-calcification temperatures: Paleothermometry for the upper water column. Earth and Planetary Science Letters 278, 324–336.

Regenberg, M., Regenberg, A., Garbe-Schönberg, D., Lea, D.W. (2014). Global dissolution effects on planktonic foraminiferal Mg/Ca ratios controlled by the calcite-saturation state of bottom waters. Paleoceanography 29, 127–142. doi:10.1002/2013PA002492.

Reißig, S., Nürnberg, D., Bahr, A., Poggemann, D.-W., Hoffmann, J. (2019). Southward displacement of the North Atlantic subtropical gyre circulation system during North Atlantic cold spells. Paleoceanography and Paleoclimatology 34. https://doi. org/10.1029/2018PA003376.

Reynolds, C.E., Richey, J.N., Fehrenbacher, J.S., Rosenheim, B.E., Spero, H.J. (2018). Environmental controls on the geochemistry of *Globorotalia truncatulinoides* in the Gulf of Mexico: Implications for paleoceanographic reconstructions. Marine Micropaleontology 142, 92–104.

Roberts, J., Gottschalk, J., Skinner, L.C., Peck, V.L., Kender, S., Elderfield, H., Waelbroeck, C., Vázquez Riveiros, N., Hodell, D.A. (2016). Evolution of South Atlantic density and chemical stratification across the last deglaciation. Proceedings of the National Academy of Sciences of the United States of America 113 (3), 514–519.

Schmidt, M.W., Chang, P., Hertzberg, J.E., Them, T.R., Ji, L., J, L., Otto-Bliesner, B.L. (2012). Impact of abrupt deglacial climate change on tropical Atlantic subsurface temperatures. Proceedings of the National Academy of Sciences of the United States of America 109 (36), 14348–14352.

Schmuker, B., Schiebel, R. (2002). Planktic foraminifers and hydrography of the eastern and northern Caribbean Sea. Marine Micropaleontology 46 (3-4), 387–403.

Steph, S., Regenberg, M., Tiedemann, R., Mulitza, S., Nürnberg, D. (2009). Stable isotopes of planktonic foraminifera from tropical Atlantic/Caribbean core-tops: Implications for reconstructing upper ocean stratification. Marine Micropaleontology 71 (1-2), 1–19. https://doi.org/10.1016/j.marmicro.2008.12.004.

Stuiver, M., Reimer, P.J., and Reimer, R.W., 2020, CALIB 8.2 [WWW program] at http://calib.org, accessed 2020-10-14.

Them, T.R., Schmidt, M.W., Lynch-Stieglitz, J. (2015). Millennial-scale tropical atmospheric and Atlantic Ocean circulation change from the Last Glacial Maximum and Marine Isotope Stage 3. Earth and Planetary Science Letters 427, 47–56.

Ujiié, Y., Garidel-Thoron, T. de, Watanabe, S., Wiebe, P., Vargas, C. de (2010). Coiling dimorphism within a genetic type of the planktonic foraminifer *Globorotalia truncatulinoides*. Marine Micropaleontology 77 (3-4), 145-153.